tively. Thus, in this case, some of the problems[51,52] in applying the Karplus relationship for analysis of $J_{1',2'}$, such as substituent perturbations, C-1'–C-2' bond lengths, etc., are minimized. Hence, we propose that the small $J_{1',2'}$ of 3'-deoxyadenosine arises from a smaller $\phi_{1',2'}$ than that of adenosine. If the Karplus plot is utilized, $\phi_{1',2'}$ will be about 120° for 2'-deoxyadenosine. A consequence of this smaller dihedral angle would be that C-2' is only slightly puckered out of the plane of the furanose ring in an *endo* fashion. Unfortunately, the other coupling constants involving protons at C-3' and C-4' were not obtainable due to the low solubility. From the stereochemical considerations, the hydrogen bond formation between the 2'-OH group and the N-3 will be much favored when the 2'-carbon is in the *endo* position than when it is not.[29] This finding, therefore, is in accord with the observation that the intramolecular hydrogen bonding was observed only for the adenosine and not for the 3'-deoxyadenosine.

In concluding, 14 purine nucleosides in aqueous solutions have been studied extensively by vapor pressure osmometry and pmr. Based on this study, several conclusions and calculations have been made on the properties of these compounds. In view of the importance of these conclusions and calculations, additional experimental observations and developments in theory are needed for further evaluation and improvement. Some of these programs are now in progress in our laboratory.

## Experimental Section

When possible, commercially available compounds of the highest degree of purity were used without further purification. Elemental analyses on compounds studied by vapor pressure osmometry were obtained from Galbraith Laboratories, Knoxville, Tenn., and from Spang Microanalytical Laboratory, Ann Arbor, Mich. These analytical values were used to determine the extent of hydration. 2'-Deoxyadenosine monohydrate (found: N, 26.06), N-6-dimethyladenosine (found: N, 24.03), and inosine [found: C, 44.56; H, 4.74; N, 20.81 ± 0.3 (average of three determinations for N)] were obtained from Sigma Chemical Co. Adenosine (found: N, 26.12) was purchased from Calbiochem. 1-Methylinosine (found: C, 46.63; H, 5.05; N, 19.60) and ribosyl-2,6-diaminopurine were obtained from Cyclo Chemical Co. Ribosylpurine samples (specified as anhydrous by the suppliers) were obtained from both Sigma and Cyclo Chemical Co. Cordycepin (3'-deoxyadenosine) was kindly provided by Dr. Robert J. Suhadolnik of the Albert Einstein Medical Center, Philadelphia, Pa. 2'-O-Methyladenosine (found: N, 24.71), N-6-methyladenosine hemihydrate (found: N, 23.96), N-6-methyl-2'-deoxyadenosine, some 1-methylinosine (found: N, 20.08), and 1-methylguanosine were prepared according to published procedure.[7,53,54] In the case of N-6-methyl-2'-deoxyadenosine, although its identity was established by ultraviolet spectrum, nmr studies, melting point, and chromatography in three solvents,[55] no satisfactory elemental analyses could be obtained despite repeated efforts. It should be noted that no elemental analyses were reported either in the paper concerning the chemical synthesis[54] or in the paper concerning enzymatic synthesis.[55] At present, it is assumed to be anhydrous in the calculation of its osmotic coefficients.

All the nucleosides used were in neutral and deionized form. The solutions in $H_2O$ or $D_2O$ were prepared by directly dissolving the weighed nucleosides without additions of salt or any other chemicals.

Vapor pressure lowering measurements were made as previously described using a Mechrolab 301A vapor pressure osmometer.[2] Nuclear magnetic resonance spectra were obtained using Varian Associates A-60 or HA-100 spectrometers. Chemical shift values are reported in cps (60 Mc) from a TMS capillary; difference values are also in cps (60 Mc). Bulk susceptibility corrections were not made, but should be less than 1 cps.

**Acknowledgment.** We are grateful to Mrs. Dorothy Sander for her assistance in obtaining many osmometry data and to Professor S. I. Chan, California Institute of Technology, and Dr. Donald Hollis, Johns Hopkins Medical School, for the reading of the manuscript. We are also indebted to Drs. Winslow Caughey and D. Hollis for the use of their A-60 spectrometer in the Department of Physiological Chemistry, The Johns Hopkins University.

(51) M. Karplus, *J. Am. Chem. Soc.*, **85**, 2870 (1963).
(52) R. V. Lemieux, J. D. Stevens, and R. R. Eraser, *Can. J. Chem.*, **40**, 1955 (1962).
(53) A. D. Broom, L. B. Townsend, J. W. Jones, and R. K. Robins, *Biochemistry*, **3**, 494 (1964).
(54) J. W. Jones and R. K. Robins, *J. Am. Chem. Soc.*, **85**, 193 (1963).
(55) D. B. Dunn and J. D. Smith, *Biochem. J.*, **68**, 627 (1958).

# Effects of Site Symmetry and Sequential Metal Binding upon Protein Titration (Zinc Insulin)

**Arthur S. Brill and John H. Venable, Jr.**

*Contribution from the Department of Molecular Biophysics, Yale University, New Haven, Connecticut 06520.* *Received December 15, 1966*

**Abstract:** A hydrogen ion titration curve for zinc insulin, in agreement with the experimental data, is computed on the basis of a model in which the metal ions are each bound to three imidazole nitrogens. The equations involved and the effects of the parameters in them are discussed in more general terms.

The hydrogen ion dissociation for metal-free and for zinc insulin are presented in two papers by Tanford and Epstein.[1,2] In the first paper, the metal-free case is quantitatively described. In the second, the titration behavior of insulin in the presence of zinc is reported to differ before and after exposure to acid or base, and

(1) C. Tanford and J. Epstein, *J. Am. Chem. Soc.*, **76**, 2163 (1954).
(2) C. Tanford and J. Epstein, *ibid.*, **76**, 2170 (1954).

the latter "reversed" curves are explained quantitatively over a limited range of pH. No attempt was made to compute a curve matching the "direct" data because of the presence of protein microcrystals in the pH range 3.5 to 8 and the belief that the crystalline nature of the precipitate would interfere critically with the passage of ions. It is now known that small molecules and ions pass freely into and out of protein crystals and react with many protein sites in much the same way as when the macromolecules are in solution.[3-5] Furthermore, recent electron paramagnetic resonance studies of cupric insulin have suggested a model for the binding of divalent metal ions in insulin crystals.[6,7] It therefore seemed appropriate to carry the analyses of Tanford and Epstein one step further and attempt to compute the direct titration curve for zinc insulin.[7] The principles employed may be of more general interest and usefulness.

## Computational Methods

The programs for computing titration curves were written in FORTRAN IV and executed on an IBM 7094. So that the curves displayed in this paper can be readily compared with those of ref 1 and 2, the number, $R$, of protons dissociated per insulin dimer (the Sanger unit of about 6000 daltons is now known to represent the monomer) is computed as a function of pH, the latter usually being incremented by 0.125 unit. The EAI Model 3440 data plotter is programmed to produce a smooth curve from these $R$-pH couples, to draw and label the coordinate axes, and to put down the experimental points (in all cases the data of Tanford and Epstein). The parameters which characterize the proton dissociation behavior have been taken directly from Table II of ref 1 which gives the number ($n_i$) of ionizing groups per dimer and the p$K$ (p$K_i$) of each type $i$. We have found, confirming the previous analysis, that the value 8.5 for the number of $\beta$- plus $\gamma$-carboxyl groups produces the minimum root mean square (rms) error in the fit of the computed titration curve of metal-free insulin to the experimental data. The relation between the electric charge per dimer, $Z$, and the electrostatic correction factor, $0.868jwZ$, was obtained from Figure 4 of ref 1, which gives $jw$ as a function of pH, and from Table I of the same paper, which, in conjunction with the relation $Z = 12 - R$, gives the dimer charge as a function of pH. Using these properties which generate the metal-free titration curve and a few assumptions about the nature of the metal binding, Tanford and Epstein were able to calculate a curve partially in agreement with the experimental data obtained from zinc insulin which had been exposed to acid or base.[2] The following reproduction of the latter calculation will serve to illustrate the main features of the computational methods employed in the present paper.

In Figure 1 are shown the experimental values (no distinction has been made between acid and base reversed points) and a curve (from pH 2 to pH 7.5) computed on the basis of the two imidazole group model of Tanford and Espstein. (In this figure and all succeeding ones, the computed titration curve for metal-free insulin is displayed for reference. The displacement of the experimental points at low pH about one-half unit below the metal-free curve may arise from promoted dissociation of protons from carboxyl groups interacting with zinc.) The calculation of $R$ *vs.* pH requires the simultaneous solution of the following four equations at each pH.

$$\log \frac{x_i}{1 - x_i} = \text{pH} - \text{p}K_i + 0.868jwZ \qquad (1)$$

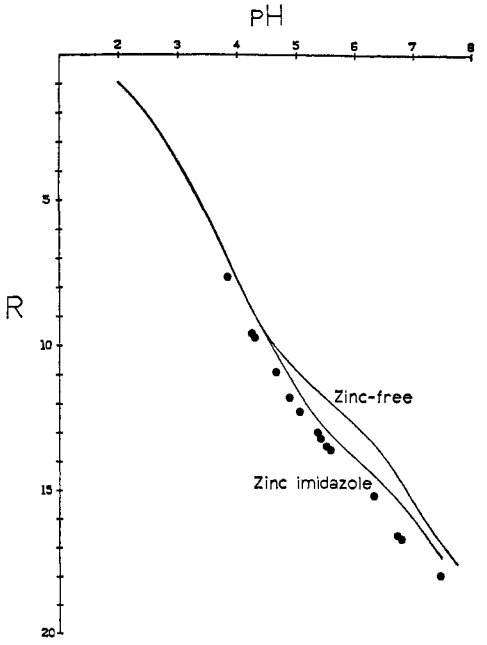


Figure 1. The hydrogen ion dissociation function of zinc insulin after exposure to acid or base: experimental points (data of Tanford and Epstein[2]) and a curve from pH 2 to 7.5 computed on the basis of double imidazole sites with log $K_{Zn} = 6.0$. The upper curve, extending to pH 8, is that of metal-free insulin and is displayed for reference.

$$\log \frac{\bar{\nu}_{Zn}}{(2 - \bar{\nu}_{Zn})(F - \bar{\nu}_{Zn})} = 2 \log x_{im} + \log P + \log K_{Zn} - 1.736jwZ \qquad (2)$$

$$R = 2\bar{\nu}_{Zn} + (4 - 2\bar{\nu}_{Zn})x_{im} + \sum_{i \neq im} n_i x_i \qquad (3)$$

$$Z = 12 + 2\bar{\nu}_{Zn} - R \qquad (4)$$

Here $x_i$ is the degree of dissociation of groups of type $i$, $\bar{\nu}_{Zn}$ is the average number of zinc ions bound per insulin dimer, $F$ is the ratio of the total number of zinc ions to the total number of insulin dimers, $x_{im}$ is the degree of dissociation of imidazole groups, $P$ is the total concentration of protein dimers, and $K_{Zn}$ is the intrinsic association constant between zinc ions and the (double) imidazole sites. Based upon a polarographic determination yielding 0.95 Zn/insulin dimer, Tanford and Epstein used for $F$ the value 1.0. However, the supplier, Eli Lilly and Co., had stated a zinc content equivalent to $F = 0.76$. This number is a reasonable one since several kinds of evidence point to a strong binding of two metal ions per three dimers[8-11] or $F = {}^2/_3$, especially in crystalline metal insulins. In response to our questions, the Chemical Research Division of Eli Lilly and Co. redetermined the zinc content of Lot No. T-2842 that was used in the experiments of ref 2, and found 0.432 and 0.429% on a moisture-free basis, confirming the 0.76 value for $F$.[12] All our calculations have therefore been made with this figure, though in no case is the *strongly* bound zinc allowed to exceed ${}^2/_3$ ion/dimer.

Since $Z$ is a monotonically decreasing function of pH, we have chosen to solve eq 1–4 by successively decrementing $Z$, usually by 0.050, starting with the value from the previous pH. The assumed value of $Z$ serves (in conjunction with a table of electrostatic corrections as a function of $Z$) to produce a value of $0.868jwZ$ so that eq 1 can be solved (once for each type of ionizing group) and eq 2 as well. $R$ is then computed from eq 3 and used in eq 4 to yield a value of $Z$ which is compared with the assumed value. The cri-

(3) F. M. Richards, *Ann. Rev. Biochem.*, **32**, 269 (1963).
(4) M. S. Doscher and F. M. Richards, *J. Biol. Chem.*, **238**, 2399 (1963).
(5) J. A. Rupley, *Biochemistry*, **3**, 1524 (1964).
(6) J. H. Venable, Jr., Thesis, Yale University, 1965.
(7) A. S. Brill and J. H. Venable, Jr., "The Biochemistry of Copper," P. Aisen, W. Blumberg, and J. Peisach, Ed., Academic Press Inc., New York, N. Y., 1966, pp 67–74.
(8) J. Schlichtkrull, *Acta Chem. Scand.*, **10**, 1455 (1956).
(9) J. Schlichtkrull, Thesis, University of Copenhagen, 1958.
(10) K. Marcker, *Acta Chem. Scand.*, **14**, 194 (1960).
(11) L. W. Cunningham, R. L. Fischer, and C. S. Vestling, *J. Am. Chem. Soc.*, 77, 5703 (1955).
(12) W. W. Bromer, personal communication.

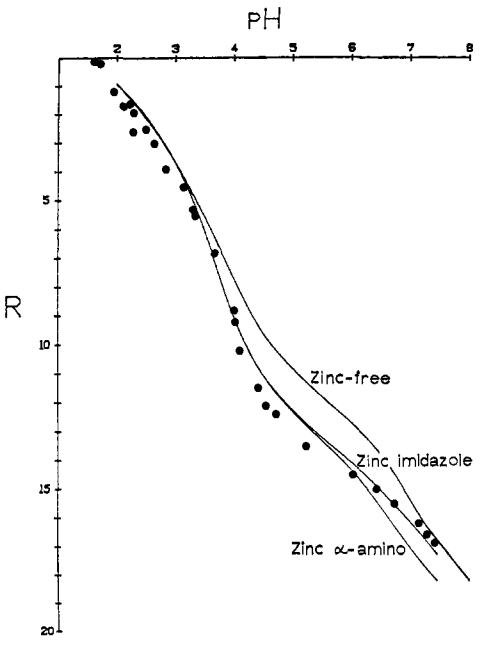


Figure 2. The direct hydrogen ion dissociation function of zinc insulin: experimental points (data of Tanford and Epstein[2]), a curve computed on the basis of triple imidazole sites with log $K_{Zn}$ = 11.2, and one on the basis of triple $\alpha$-amino sites with log $K_{Zn}$ = 14.3.

terion of solution is the minimization of the difference between the assumed and calculated values of $Z$. It can be seen in Figure 1, as in ref 3, that the model fails above pH 6.5. While the fit can be improved, the properties of the "reversed" titration curve will not be pursued further here since we have treated this case mainly to demonstrate methods and wish to use Figure 1 as it is, with log $K_{Zn}$ = 6.0, in the discussion.

## The Threefold Axis

Evidence for the location of metal ions on the threefold axis of rhombohedral insulin crystals has been summarized.[6,7] In particular, electron paramagnetic resonance spectra from single crystals of cupric insulin are characteristic of the cupric ion in a trigonal site and show, furthermore, that each ion is bound to three nitrogens. These nitrogens could belong to imidazole groups or to $\alpha$-amino groups. Equation 2 is readily modified so that two sites, each consisting of three imidazole or three amino nitrogens, per three dimers are involved in metal binding—that is, $^2/_3$ site/dimer

$$\log \frac{\bar{\nu}_{Zn}}{(^2/_3 - \bar{\nu}_{Zn})(F - \bar{\nu}_{Zn})} = 3 \log x_j + \log P + \log K_{Zn} - 1.736jwZ \quad (5)$$

where $j$ = imidazole or $\alpha$-amino. The zinc in excess of $^2/_3$ ion/dimer remains unbound in this approximation. Equation 3 also requires modification.

$$R = 3\bar{\nu}_{Zn} + (4 - 3\bar{\nu}_{Zn})x_j + \sum_{i \neq j} n_i x_i \quad (6)$$

Equation 4 remains as before. The equations are solved simultaneously as described in the Computational Methods. It is important to note that, in order for the curves to reflect no new assumptions beyond that of the trigonal site, the parameters $n_i$ and $pK_i$ and the function $jwZ$ are taken exactly as in ref 1, though the latter function is unlikely to be identical for the zinc and metal-free cases. There remains only one parameter, $K_{Zn}$, which can be adjusted to improve the fit of the computed curves to the experimental data. In Table I is shown the behavior of the rms difference between the computed and experimental points from pH 3.66 to pH 7.40 as a function of log $K_{Zn}$. The optimum log $K_{Zn}$ for the trigonal imidazole site is 11.2, or 3.7/ligand, a figure which is high for zinc–imidazole binding. For the trigonal $\alpha$-amino site, the optimum log $K_{Zn}$ is 14.3, or 4.8/ligand, also a high value for an amino–zinc link in the absence of chelation.

In Figure 2 are shown the "best" curves (pH 2–7.5) for the imidazole and $\alpha$-amino cases. The two types of site fit the data equally well up to pH 6. However the $\alpha$-amino curve diverges from the experimental data above pH 6.5 while the histidine curve remains in agreement. This fact is shown quantitatively by the rms errors of Table I. The failure of the trigonal

**Table I.** Rms Differences between Computed and Experimental Dissociation (in Protons per Dimer) for the 14 Points from pH 3.66 to pH 7.40

| Log $K_{Zn}$ | Rms difference | Log $K_{Zn}$ | Rms difference |
|---|---|---|---|
| Imidazole Site | | $\alpha$-Amino Site | |
| 10.6 | 0.53 | 13.7 | 0.79 |
| 10.9 | 0.49 | 14.0 | 0.76 |
| 11.2 | 0.47 | 14.3 | 0.75 |
| 11.5 | 0.48 | 14.6 | 0.76 |
| 11.8 | 0.49 | 14.9 | 0.77 |

$\alpha$-amino site could have been predicted had we understood the implications of the tangency of the metal-free and zinc insulin titration curves at pH 7.3. Since the p$K$ of the $\alpha$-amino protons is about 7.5, in metal-free insulin these are being actively titrated at pH 7.3, while the imidazole protons, with a p$K$ of 6.4, have largely been titrated by pH 7.3. In the zinc insulin model which has half of the $\alpha$-amino groups (those bound to metal) with an apparent p$K$ of about 4.5, these groups have lost their protons well below 7.3 and hence the titration curve must diverge from the metal-free curve.[13] The imidazole model behaves satisfactorily at pH 7.3 since the amino protons are unaffected and the imidazole protons will have dissociated in both metal-free and zinc insulin. (The divergence of the metal-free and zinc curves above pH 7.5 arises from the dissociation of protons from the hydration sphere of the zinc.)

One may conclude from the evidence presented in this section that: (1) the trigonal imidazole site explains the hydrogen ion titration curve of crystalline zinc insulin in the pH region 3.5–7.5; (2) a site consisting of $\alpha$-amino groups fails.

A point which requires further consideration is the unusually large value for the association constant for zinc.

## Sequential Metal Binding

In the approximation of the preceding section the two trigonal sites associated with three insulin dimers are treated identically. That is, the occupation of one of the sites by a zinc ion is not considered to have an effect upon the association of another zinc ion to the second

(13) Zinc–$\alpha$-amino interaction is a likely explanation of the titration behavior of acid- or base-treated insulin, shown by the data points of Figure 1.

site. A plausible model for the metal–insulin interaction is one in which the metal serves as a link between three insulin dimers.[6,14] In this case the decrease in entropy upon formation of the first site must be the greater part of the total entropy decrease in bringing the three protein dimers from an unorganized state to the final configuration. Whence, to a better approximation, one may treat the binding of the metal ions as a two-step process: (1) the coordination of the first zinc ion to an insulin trigonal site occurs in much the same way as to three independent small molecule ligands; (2) then, because they are connected (by lengths of polypeptide chains) to the first site, the coordinating atoms of the second site have a relatively high probability of being in the proper position to bind a metal ion, and hence the association constant for the binding of the second ion will be greater than for the first. One can view the formation of the first complex as producing a chelation property in the second site, but there is less order in the polypeptide "claws" than in those of the usual chelating agents.

The translation of this picture of sequential metal binding into mathematical terms is straightforward. If we let $\bar{\nu}_1$ be the number (per dimer) of zinc ions bound to singly occupied dimers and $\bar{\nu}_2$ to doubly occupied dimers, then the concentration of free zinc is $(F - \bar{\nu}_1 - \bar{\nu}_2)$. The concentration of sites on dimers entirely free of zinc is $(^2/_3 - 2\bar{\nu}_1 - \bar{\nu}_2)P$ since (1) in the absence of metal, there is $^2/_3$ site/dimer; (2) occupancy by a single zinc ion also removes the second site on the same dimer as being in the class under consideration; (3) each double occupancy removes two sites. The concentration of sites which are entirely free of both protons and zinc is then $(^2/_3 - 2\bar{\nu} - \bar{\nu}_2)x_{im}{}^3P$. (We are now restricting the model to imidazole groups, having rejected $\alpha$-amino sites in the preceding section.) It follows that the association of the first zinc ion is governed by the relation

$$\log \frac{\bar{\nu}_1}{(^2/_3 - 2\bar{\nu}_1 - \bar{\nu}_2)(F - \bar{\nu}_1 - \bar{\nu}_2)} = 3 \log x_{im} + \log P + \log K_1 - 1.736jwZ \quad (7)$$

where $K_1$ is the intrinsic association constant for this equilibrium. The association of the second zinc ion is treated in terms of an equilibrium with singly occupied complexes

$$\log \frac{\bar{\nu}_2}{\bar{\nu}_1(F - \bar{\nu}_1 - \bar{\nu}_2)} = 3 \log x_{im} + \log P + \log K_2 - 1.736jwZ \quad (8)$$

Equation 1 remains valid. Equations 6 and 4 are modified as follows.

$$R = 3(\bar{\nu}_1 + \bar{\nu}_2) + (4 - 3(\bar{\nu}_1 + \bar{\nu}_2))x_{im} + \sum_{i \neq im} n_i x_i \quad (9)$$

$$Z = 12 + 2(\bar{\nu}_1 + \bar{\nu}_2) - R \quad (10)$$

The simultaneous solution of eq 7 and 8 starts with the assumption of a value for $\bar{\nu}_1$ (initially zero). Equation 8 then yields $\bar{\nu}_2$ (subject to a maximum value of $^2/_3 - \bar{\nu}_1$) which is used in eq 7 to calculate $\bar{\nu}_1$. The assumed value of $\bar{\nu}_1$ is repeatedly incremented (by 0.0005 or less) until the difference between it and the calculated value reaches a minimum.

(14) K. Marcker and J. Graae, *Acta Chem. Scand.*, **16**, 41 (1962).

In Table II is given a matrix of rms errors corresponding to log $K_1$ and log $K_2$ values in the regions of "best fit." The important features which are exhibited by these calculations are as follows: (1) the log $K_1$–log $K_2$ couples corresponding to the trough of rms errors average to approximately the optimum log $K_{Zn}$ value (11.2) of the preceding section; (2) when $K_1 = K_2$, the computed and experimental data agree to the same extent as in Table I (the calculated curves in this case are identical with those calculated in the preceding section with $K_{Zn} = K_1 = K_2$, which provides an internal check of the computation); (3) there is some improvement in the agreement of computed and experimental data when $K_2 > K_1$.

**Table II.** Rms Differences between Computed and Experimental Dissociation (in Protons per Dimer) for the 14 Points from pH 3.66 to pH 7.40[a]

| Log $K_1$ | Rms differences for log $K_2$ | | | | | | | |
|---|---|---|---|---|---|---|---|---|
| | 11.2 | 11.5 | 11.8 | 12.1 | 12.4 | 12.7 | 13.0 | 13.3 |
| 7.9 | | | | | 0.61 | 0.54 | 0.51 | 0.50 |
| 8.2 | | | | | 0.56 | 0.53 | 0.50 | 0.48 |
| 8.5 | | | | | 0.52 | 0.49 | 0.46 | 0.45 |
| 8.8 | | | | | 0.48 | 0.47 | 0.45 | 0.45 |
| 9.1 | 0.62 | 0.57 | 0.52 | 0.49 | 0.47 | 0.46 | 0.45 | 0.46 |
| 9.4 | 0.57 | 0.53 | 0.49 | 0.46 | 0.45 | 0.45 | 0.46 | 0.47 |
| 9.7 | 0.53 | 0.49 | 0.47 | 0.45 | 0.45 | 0.46 | 0.47 | 0.48 |
| 10.0 | 0.50 | 0.47 | 0.46 | 0.45 | 0.46 | 0.47 | 0.49 | 0.50 |
| 10.3 | 0.48 | 0.46 | 0.46 | 0.46 | 0.47 | 0.48 | 0.50 | 0.52 |
| 10.6 | 0.47 | 0.46 | 0.46 | 0.47 | 0.48 | 0.50 | 0.51 | 0.53 |
| 10.9 | 0.47 | 0.46 | 0.47 | 0.48 | | | | |
| 11.2 | 0.47 | 0.47 | 0.48 | 0.49 | | | | |
| 11.5 | 0.48 | 0.48 | 0.49 | 0.50 | | | | |
| 11.8 | 0.48 | 0.49 | 0.49 | 0.51 | | | | |

[a] Sequential zinc binding is characterized by the intrinsic association constants $K_1$ and $K_2$ to the trigonal imidazole sites.

The latter improvement is concentrated in the pH region 3.7–4.5 where the marked change in slope which characterizes the experimental curve is more faithfully reproduced.

According to the viewpoint of sequential metal binding stated earlier, we therefore suggest that the first zinc ion is bound with an association constant which is in the range normally found for zinc–imidazole interaction, about $10^9$ for three coordinate links, and the second zinc ion is bound about $10^4$ times more strongly. An explanation can now be given of the point raised at the end of the preceding section, which concerned the unusually large value of the optimum log $K_{Zn}$. The latter is shown to be the average of log $K_1 \approx 9$ and log $K_2 \approx 13$, and hence substantially greater than the "expected" value (about $K_1$ alone).

## Discussion

When a metalloprotein is the subject of an investigation (*e.g.*, single-crystal X-ray diffraction or electron paramagnetic resonance orientation study) which reveals molecular symmetries, these symmetry elements can be related to the hydrogen ion dissociation behavior in explicit mathematical form. For example, the cases expressed by the pairs of eq 2,3 and 5,6 can be generalized to metal ions on an $n$-fold axis bound to polymeric

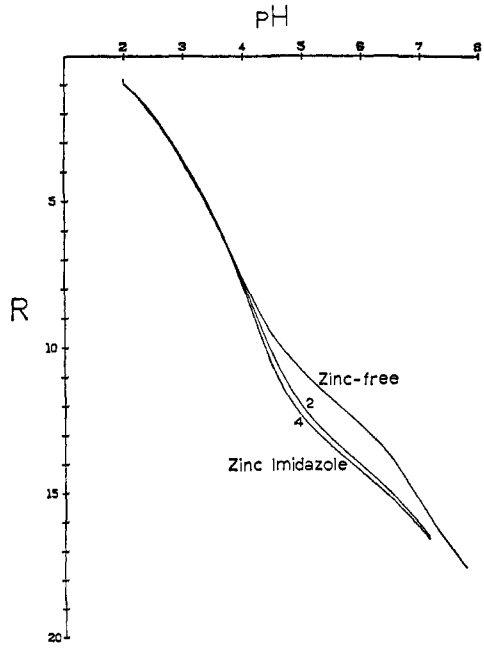


Figure 3. Hydrogen ion dissociation functions for insulin in which zinc is bound to triple imidazole sites with log $K_{Zn}$ = 9.0. The steeper curve has four such sites per six Sanger units; the other curve, two.

chains of a symmetry which generates $m$ equivalent sites along the axis.

$$\log \frac{\bar{\nu}}{((m/n) - \bar{\nu})(F - \bar{\nu})} = n \log x_j + \log P + n \log k + f(z) \quad (11)$$

$$R = n\bar{\nu} + (n_j - n\bar{\nu})x_j + \sum_{i \neq j} n_i x_i \quad (12)$$

where $\bar{\nu}$, $F$, $x_i$, and $P$ have the same meaning as before, $k$ is the effective intrinsic association constant for a single metal–ligand link (sequential binding is not explicitly treated in this formalism), and f($z$) is the appropriate electrostatic correction function.

It can be shown analytically that, in the region where the change in metal bound with pH is greatest, the buffering capacity d$R$/dpH is proportional to $n^2$. Comparisons of curve 2 ($n$ = 1, log $K_{Zn}$ = log $k$ = 3, $F$ = 1) with curve 3 ($n$ = 2, $^1/_2$ log $K_{Zn}$ = log $k$ = 3, $F$ = 1) of Figure 3 of Tanford and Epstein,[2] and of Figure 1 ($n$ = 2, $^1/_2$ log $K_{Zn}$ = log $k$ = 3, $F$ = 0.76) with the $m$ = 2 curve of Figure 3 ($n$ = 3, $^1/_3$ log $K_{Zn}$ = log $k$ = 3, $F$ = 0.76) of this paper will serve to illustrate the marked effect which the symmetry parameter $n$ has upon the shape of the titration curve. The decrease of the apparent p$K$ of the ionizing groups to which the metal ions are bound with increasing $n$ should also be noted.

The number, $m$, of equivalent sites has much less influence than $n$ upon the proton dissociation function, and this influence is significant only when $m/n \lesssim F$. The effect of increasing $m$, demonstrated in Figure 3, is qualitatively the same as increasing $n$, strengthening the average buffer capacity, and lowering the apparent p$K$. The maximum number of metal ions bound per polymer chain is equal to the smaller of $m/n$ and $F$, hence increases to $F$ as $m/n$ changes from below to above this value.

While $m > 1$ signifies the existence of equivalent sites, the successive attachments of metal ions to these sites are not all equivalent. The case $m$ = 2, treated in the section on sequential metal binding, is readily extended to larger values of $m$. A likely situation is one in which the association constant is the same for all but the first metal ion, though, for large $m$, one can imagine "internal sites" being sterically hindered as $\bar{\nu}$ approaches $m/n$. The value of $F$ in relation to $m/n$ determines whether or not such saturation is possible. In general, sequential metal binding will sharpen the onset of the region of maximum buffering capacity.

Implicit assumptions underlying this discussion are that structural information obtained from proteins in the solid state applies to these macromolecules in solution, and that the thermodynamic parameters which characterize proton dissociation are essentially invariant under this phase transition. In the case of zinc insulin, the considerable agreement of the computed dissociation function (for a model based on data from crystals) with the experimental titration curve (from a two-phase system) supports these assumptions and also indicates that the electrostatic correction function may not differ greatly from phase to phase.

**Acknowledgments.** We are pleased to thank Patricia H. Brill for programming the computations, Dr. W. W. Bromer and his colleagues at the Chemical Research Division of Eli Lilly and Co. for the zinc analyses, and Dr. H. Brintzinger for a valuable discussion.

The use of the Yale Computer Center facilities for the development of programs to compute and display titration curves was made possible by a National Science Foundation Grant to Yale University for the support of unsponsored research. Application of these programs to the analysis of metal–protein interactions is supported by U. S. Public Health Service Research Grant GM-09256 from the Division of General Medical Sciences.